Separation Science and Technology
Publication details, including instructions for authors and subscription information:
http://www.informaworld.com/smpp/title~content=t713708471

Lysine Adsorption on Cation Exchange Resin. I. Ion Exchange Equilibrium and Kinetics

Hidetada Nagai[ab]; Giorgio Carta[a]
[a] Department of Chemical Engineering, University of Virginia, Charlottesville, Virginia, USA [b] Technology and Engineering Laboratory, Ajinomoto, Co., Inc., Kawasaki-ku, Kawasaki-shi, Japan

Online publication date: 08 July 2010

To cite this Article Nagai, Hidetada and Carta, Giorgio(2004) 'Lysine Adsorption on Cation Exchange Resin. I. Ion Exchange Equilibrium and Kinetics', Separation Science and Technology, 39: 16, 3691 — 3710
To link to this Article: DOI: 10.1081/SS-200041091
URL: http://dx.doi.org/10.1081/SS-200041091

SEPARATION SCIENCE AND TECHNOLOGY
Vol. 39, No. 16, pp. 3691–3710, 2004

Lysine Adsorption on Cation Exchange Resin. I. Ion Exchange Equilibrium and Kinetics

Hidetada Nagai[1,2] and Giorgio Carta[1,*]

[1]Department of Chemical Engineering, University of Virginia, Charlottesville, Virginia, USA
[2]Ajinomoto, Co., Inc., Technology and Engineering Laboratory, Kawasaki-ku, Kawasaki-shi, Japan

ABSTRACT

Ion exchange equilibria and kinetics are determined for lysine adsorption on the strong acid cation exchanger Dowex HCR-W2. Average ion exchange selectivity coefficients of 5.0 g/cm^3 and 0.75 are obtained for the ion exchange of divalent and monovalent cationic lysine with hydrogen ion, respectively, while values of 1.5 and 1.9 are obtained for the exchange of ammonium and potassium with hydrogen ion. A model based on these binary ion exchange measurements and accounting for the solution equilibria is then developed to predict lysine adsorption over a broad range of conditions. Similarly, resin phase diffusivities are determined by fitting batch binary ion-exchange data with a mass transfer

*Correspondence: Giorgio Carta, Department of Chemical Engineering, University of Virginia, Charlottesville, VA, USA; E-mail: gc@virginia.edu.

DOI: 10.1081/SS-200041091 0149-6395 (Print); 1520-5754 (Online)

model based on the Nernst-Planck equations. Diffusivities of divalent cationic lysine, monovalent cationic lysine, ammonium ion, and potassium ion are 0.05×10^{-6}, 0.20×10^{-6}, 1.6×10^{-6}, and $1.9 \times 10^{-6}\,cm^2/s$, respectively. Finally, a general rate model incorporating ion exchange and solution equilibria is developed to predict batch adsorption and desorption of lysine using these diffusivity values over a broad range of conditions.

Key Words: Ion exchange equilibria; Ion exchange kinetics; Zwitterionic species; Lysine adsorption.

INTRODUCTION

Ion exchange plays a central role in the industrial production of amino acids and is especially critical in the manufacture of lysine, one of the largest industrial fermentation products.[1] Amino acids are zwitterionic and can be positively charged, neutral, or negatively charged depending on the solution pH. As a result, amino acids that are bound to a cation exchange resin at low pH can be desorbed by raising the pH to a value where the amino acid becomes negatively charged. For practical and economic reasons, ammonia is often used for this purpose. Rational design and optimization of such ion exchange processes requires a knowledge of both the ion exchange equilibrium, which determines the maximum resin loading capacity; and the ion exchange kinetics; which determine the dynamic binding capacity as a function of flow rate as well as the time and amount of desorbent required for elution. As a result, a quantitative understanding of these two factors is critical.

The ion exchange equilibrium of several neutral and acidic amino acids on cation exchangers has been investigated by a number of authors.[2–7] As shown by these authors, amino acid adsorption on cation exchangers occurs via the stoichiometric exchange of amino acid cations. Accordingly, there is no significant binding of the zwitterionic species indicating that the proximity of positive and negative charges in the zwitterion prevents a favorable electrostatic interaction with the negatively charged functional groups in the resin. Equilibrium models also have been developed, including models based on the homogeneous and heterogeneous mass action law for ion exchange[2–6,8] and activity coefficients–based models where partitioning of all cationic, anionic, and zwitterionic species between the resin and the solution phase is described explicitly.[7]

The kinetics of ion exchange of certain neutral amino acids in cation exchange resins has also been studied. The intraparticle diffusivities of the amino acids alanine, α-aminobutyric acid, leucine, and phenylalanine were determined by Jones and Carta[9] for sulfonated poly(styrene-divinylbenzene)

(DVB) cation exchange resins with degrees of cross-linking between 2% and 10%. For resins with 8% cross-linking, these authors found diffusivities between 0.01×10^{-5} and $0.001 \times 10^{-5}\,cm^2/s$, corresponding to ratios of resin and solution diffusivity, D/D^0, in the range 0.07 to 0.005. These results suggest that diffusion of the bulkier amino acids in these resins is hindered to a much greater extent than that of small inorganic ions, for which D/D^0 is around 0.1.[10,11] A similar result was obtained by Melis et al.[6] for the diffusivity of proline in an 8% DVB resin ($D/D^0 = 0.03$). Jones and Carta[9] also provided an empirical correlation to predict amino acid diffusivities in cation exchange resins as a function of their molar volume.

Although no data seems to be available in the literature on the resin-phase diffusivity of divalent amino acid cations, the diffusivities of divalent inorganic ions are known to be much smaller than are the corresponding values for monovalent cations, or about 1/100 of the solution diffusivity value.[10,11] As a result, the resin-phase diffusivity of amino acids with a positively charged side chain can also be expected to be substantially smaller than that for the cations of amino acids with uncharged side chain.

Ion Exchange Lysine

Limited data are available in the literature on the ion exchange of lysine or other divalent amino acids. Kawakita et al.[12] studied the equilibrium uptake of lysine on cation exchange resins with degree of cross-linking between 4% and 16% in ammonium form. Uptake isotherms were obtained at high pH (~6), where only monovalent lysine and ammonium ion are present, and at low pH (pH ~ 0.8–1), where only divalent lysine is present. The ion exchange equilibrium of lysine with an 8% cross-linked resin in hydrogen form has also been studied by Dye et al.[2] These authors considered the exchange of mono valent/divalent lysine mixtures at intermediate pH values but only for the hydrogen form of the resin.

No values of the resin phase diffusivity of lysine cations seem to have been reported in the literature, although the ratio D/D^0 can be estimated from the correlation of Jones and Carta.[9] The solution diffusivity of lysine, D^0, can be estimated from the Wilke-Chang equation[13] to be $0.69 \times 10^{-5}\,cm^2/s$ using a molar volume of $171\,cm^3/mol$ based on the LeBas volumes. For an 8% cross-linked resin in hydrogen form, the Jones and Carta correlation yields $D/D^0 = 0.031$ or $D_{Lys^+} = 2.1 \times 10^{-7}\,cm^2/s$. The resin phase diffusivity of divalent lysine cannot be estimated from this correlation. However, based on the known behavior of inorganic cations, we can expect $D_{Lys^{++}}$ to be substantially smaller.

The objective of this paper is threefold. The first objective is to provide a consistent set of ion-exchange equilibrium data for a system comprising

lysine, ammonia, potassium, and hydrogen ion over a broad range of pH. Data for several binary ion exchange equilibria are obtained and equilibrium constants are derived taking into account the ionic distribution of lysine and ammonia species in solution. The second objective is to characterize the kinetics of ion exchange by performing batch experiments for conditions where monovalent lysine, divalent lysine, and their mixtures are present. Finally, the third objective is to develop a model to describe ion exchange equilibria and kinetics in these multicomponent systems. The application of these models to predict the behavior of single column systems is discussed in Part II of this work while the application to multicolumn merry-go-round systems for lysine recovery is discussed in Part III.

MATERIALS AND METHODS

The resin used in this work is Dowex HCR-W2 (Dow Chemical Co., Midland, MI), a typical gel-type poly(styrene-divinylbenzene) cation exchanger with a nominal DVB content of 8% and sulfonic acid functional groups. The mean particle diameter of the hydrogen form resin is 714 μm as determined from microphotographs. The dry weight of the resin in H-form is 0.48 g dry/g of hydrated resin, while the density of the resin beads in hydrogen form is 0.65 g dry/cm^3 of hydrated particle. The total ion exchange capacity of the resin was determined to be 5.3 ± 0.2 mequiv/g dry H-form resin. These values are consistent with previous determinations in our laboratory.[4]

L-lysine was obtained from Ajinomoto Co., Inc. (Raleigh, NC). Potassium chloride was purchased from Sigma Chemical. Co. (St. Louis, MO), while ammonium hydroxide and ammonium chloride were purchased from Fisher Scientific Co. (Pittsburgh, PA). Actual lysine fermentation broths contain many cationic impurities. However, potassium can be used as a representative interfering species.[14] Thus potassium chloride and potassium hydroxide were also obtained from Fisher and used in this work.

Ion exchange equilibria were determined by a batch method. Solutions containing lysine, ammonia, and potassium ion were prepared with constant concentrations of chloride ion using stock solutions of free-base lysine, lysine hydrochloride, ammonium hydroxide, potassium chloride and hydrochloride (HCL). Aliquots of these solutions (10 mL) were than added to test tubes containing various amounts of wet H-form resin, which were centrifuged at 3000 rpm for 10 min in a perforated centrifuge tube to remove interstitial water. The tubes were rotated for 4 hours, which was sufficient to reach equilibrium as indicated by batch experiments where the solution concentrations were monitored as a function of time. The amounts adsorbed by the resin were calculated from the residual composition of the solution phase using a material balance.

The HPLC analyses were used to determine the concentrations of ammonia, lysine, and potassium ion with an Alltech Associates, Inc. (Deerfield, IL) Universal Cation ion-exchange column (4.6 × 100 mm). The mobile phase was a 6 mM aqueous solution of methane sulfonic acid (Sigma Chemical Co., St., Louis, MO) and detection was with a waters Model 430 conductivity detector (Waters, Milford, MA) without ion suppression. The sample size was 5 μL.

Ion exchange rates were measured in a 100 mL agitated and thermostated glass vessel at 22 ± 2°C. The vessel is equipped with a magnetically driven Teflon impeller, which rests on the vessel's conical bottom preventing damage to the particles while ensuring their complete suspension and mixing of the solution. The agitation rate was approximately 300 rpm. To conduct the experiments, samples of solutions containing a selected counterion were added to the vessel and allowed to reach thermal equilibrium. Preweighed resin samples were then quickly added and the course of the exchange process monitored by taking 0.5 mL samples and analyzing them by HPLC, as described previously. Ammonium and sodium ion exchange kinetics experiments were also followed by continuously monitoring the electrical conductivity of the solution using a conductivity meter (Orion Research, Model 135A) with a probe dipped in the agitated vessel.

EXPERIMENTAL RESULTS AND MODELING

Ion Exchange Equilibria

In solution, lysine and ammonia dissociate according to the following reactions and equilibrium ratios:

$$\mathrm{Lys}^{++} \rightleftharpoons \mathrm{Lys}^{+} + \mathrm{H}^{+}, \quad K_1 = \frac{C_{Lys^+} C_{H^+}}{C_{Lys^{++}}}$$

$$\mathrm{Lys}^{+} \rightleftharpoons \mathrm{Lys}^{\pm} + \mathrm{H}^{+}, \quad K_2 = \frac{C_{Lys^\pm} C_{H^+}}{C_{Lys^+}}$$

$$\mathrm{Lys}^{\pm} \rightleftharpoons \mathrm{Lys}^{-} + \mathrm{H}^{+}, \quad K_3 = \frac{C_{Lys^-} C_{H^+}}{C_{Lys^\pm}}$$

$$\mathrm{NH}_4^{+} \rightleftharpoons \mathrm{NH}_3 + \mathrm{H}^{+}, \quad K_N = \frac{C_{NH_3} C_{H^+}}{C_{NH_4^+}}$$

The distribution of the different species is a function of pH and is shown in Fig. 1, based on *K*-values from Ref.[15]. It can be seen that at pH values below 1 lysine exists predominately in divalent cationic form, while at pH values above 4, monovalent lysine form is the dominant cationic form.

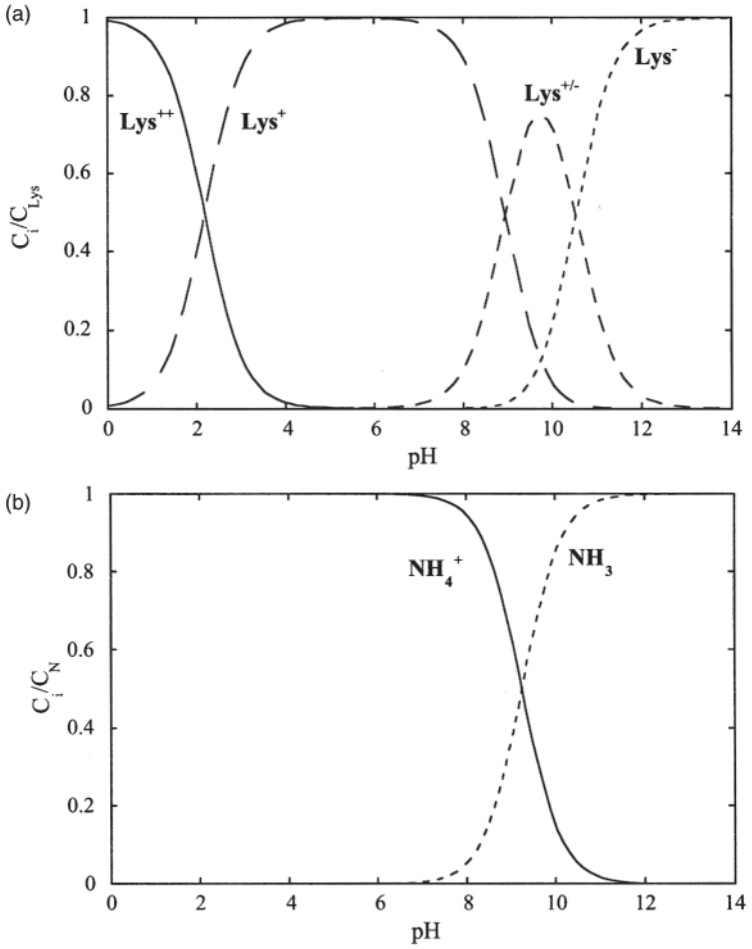

Figure 1. Distribution of lysine (a) and ammonia (b) species in solution as a function of pH calculated with values of $pK_1 = 2.18$, $pK_2 = 8.95$, and $pK_3 = 10.53$ for lysine ($pI = 9.74$) and $pK_N = 9.25$ for ammonia from Ref.[15].

Between pH values of 1 and 4, monovalent and divalent cationic forms coexist. Ammonia, on the other hand, is a stronger base and completely dissociates to NH_3 above pH 10.5.

The lysine adsorption isotherm by the hydrogen form resin over different ranges of solution pH is shown in Fig. 2a. These experiments were done at three different but constant levels of the chloride co-ion, namely 0 M,

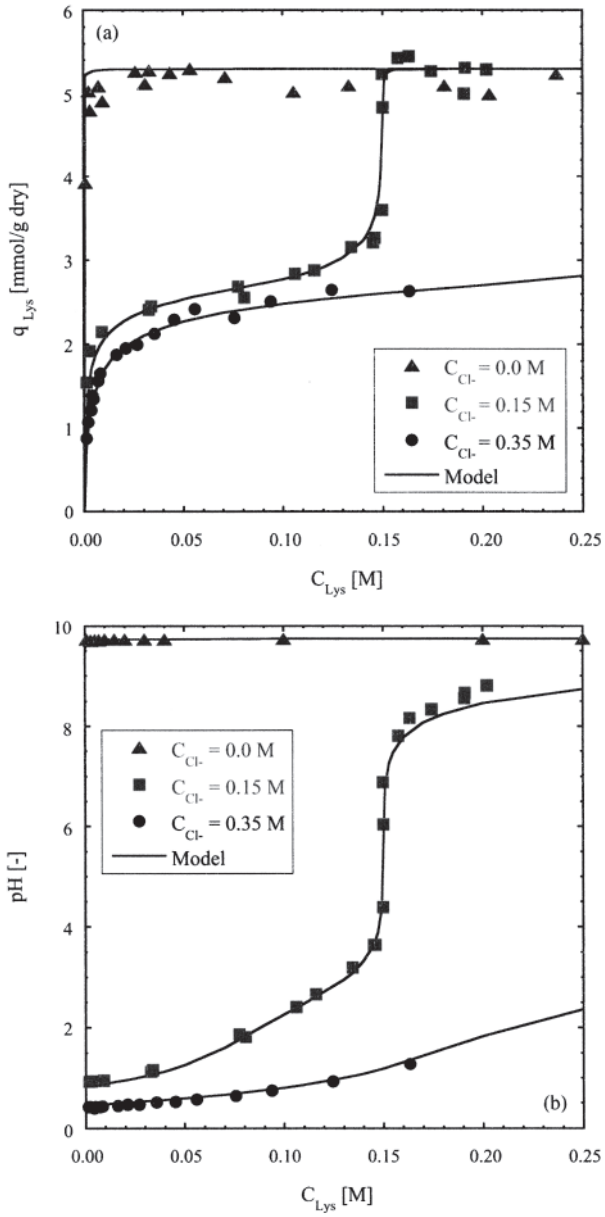

Figure 2. Adsorption isotherms for lysine on hydrogen form resin with $C_{Cl^-} = 0$ M, 0.15 M, and 0.35 M. (a) Amount of lysine adsorbed; (b) solution pH. Lines are predicted from equilibrium model.

0.15 M, and 0.35 M. As a result, the pH varied with lysine concentration for each set as shown in Fig. 2b. This was not the case, however, for 0 M chloride. For these conditions, the pH was always close to the isoelectric point of lysine (~9.74) as no other buffering species were present. As is seen in Fig. 2a, at the high chloride concentration, the lysine adsorption isotherm is favorable and approaches a maximum capacity close to one half of the total resin capacity. For these conditions, the pH remains low and lysine uptake occurs via the stoichiometric exchange of divalent lysine cations and hydrogen ion. Near the isoelectric point (0 M chloride), however, the isotherm becomes practically irreversible with an uptake capacity close to the total resin capacity. Here the uptake process is controlled by the exchange of monovalent lysine cations and hydrogen ion. For these conditions, since the hydrogen ion concentration is very low, the lysine uptake isotherm is nearly rectangular. Finally, at the intermediate chloride concentration, the uptake isotherm is S-shaped going from the favorable divalent lysine-hydrogen ion exchange behavior at low lysine concentration to the monovalent lysine-hydrogen ion exchange behavior at high lysine concentrations. For intermediate lysine concentrations both exchange reactions take place.

In order to model this complicated behavior, it is necessary to analyze the results for the individual binary ion exchange equilibria. These are shown in Fig. 3a–d plotted in the usual form in terms of ionic fractions for the binary systems Lys^{++}/H^+, Lys^+/NH_4^+, NH_4^+/H^+ and K^+/H^+. It should be noted that it is not possible to obtain reliable data for the Lys^+/H^+ exchange equilibrium in a direct way since at the pHs required to have lysine exclusively in monovalent cationic form, the hydrogen ion concentration is so low that the lysine uptake isotherm is practically irreversible. However, the equilibrium for this binary can be extracted by comparing the data for the Lys^+/NH_4^+ and NH_4^+/H^+ binaries.

As seen in Fig. 3a, the Lys^{++}/H^+ exchange is highly favorable consistent with the behavior of divalent inorganic cations.[10] The exchange of ammonium ion and potassium ion for hydrogen ion is also favorable although the selectivity is not as high as for divalent lysine, since the electro selectivity effect is not present in these monovalent exchanges. On the other hand, the Lys^+/NH_4^+ is distinctly unfavorable.

The relevant binary ion exchange reactions are given by the following equations:

$$2\,RH + Lys^{++} \rightleftharpoons R_2Lys + 2H^+$$
$$RNH_4 + Lys^+ \rightleftharpoons RLys + NH_4^+$$
$$RH + NH_4^+ \rightleftharpoons RNH_4 + H^+$$
$$RH + K^+ \rightleftharpoons RK + H^+$$

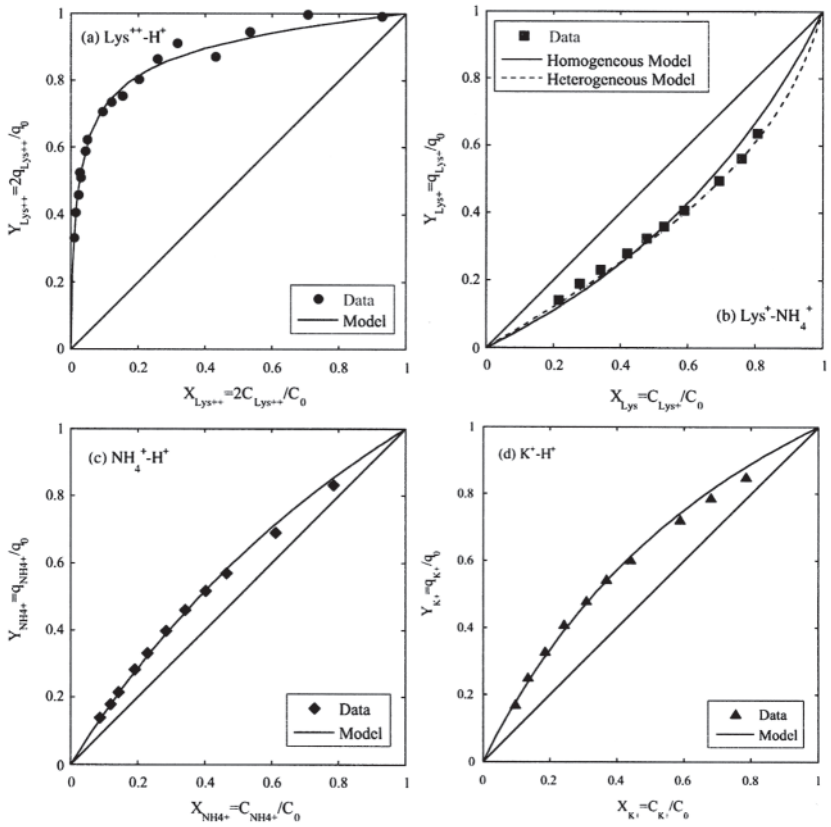

Figure 3. Equilibria for: (a) divalent lysine-hydrogen ion exchange with $C_{Cl^-} = 0.56\,\text{M}$; (b) monovalent lysine-ammonium ion exchange with $C_{Cl^-} = 0.2\,\text{M}$; (c) ammonium ion-hydrogen exchange with $C_{Cl^-} = 0.28\,\text{M}$; and (d) potassium ion-hydrogen exchange with $C_{Cl^-} = 0.28\,\text{M}$.

The corresponding mass action law selectivity coefficient expressions are

$$S_{Lys^{++}/H^+} = \frac{q_{Lys^{++}} C_{H^+}^2}{q_{H^+}^2 C_{Lys^{++}}} \tag{1}$$

$$S_{Lys^{+}/NH_4^+} = \frac{q_{Lys^{+}} C_{NH_4^+}}{q_{NH_4^+} C_{Lys^{+}}} \tag{2}$$

$$S_{NH_4^+/H^+} = \frac{q_{NH_4^+} C_{H^+}}{q_{H^+} C_{NH_4^+}} \tag{3}$$

$$S_{K^+/H^+} = \frac{q_{K^+} C_{H^+}}{q_{H^+} C_{K^+}} \tag{4}$$

In these equations C_i and q_i are the solution and the resin-phase concentrations, respectively. The selectivity coefficient for the monovalent lysine-hydrogen ion exchange can be obtained by combining Eqs. 2 and 3, yielding

$$S_{Lys^+/H^+} = \frac{q_{Lys^+} C_{H^+}}{q_{H^+} C_{Lys^+}} = S_{Lys^+/NH_4^+} \times S_{NH_4^+/H^+} \tag{5}$$

Average selectivity values obtained by fitting Eqs. 1–4 to the data are summarized in Table 1 and curves calculated accordingly are shown in Fig. 3. It can be seen that these constant-selectivity curves provide a good fit of the data in most cases. An exception is the exchange of monovalent lysine for which the selectivity decreases significantly as the ionic fraction of lysine in the resin phase increases. This effect has also been seen for the exchange of other monovalent amino acids.[3–5,7] While thermodynamic nonidealities are probably contributing factors, steric or size exclusion effects and adsorbate-adsorbate interactions are likely more significant causes of this behavior. In fact, it should be noted that full saturation of the resin with monovalent lysine requires the resin to contain 5.3 mmol/g dry resin or about 0.77 g/g dry resin. Since the resin in H-form contains approximately only 0.5 g of water per g of dry resin, it is not surprising that deviations from ideality due to steric hindrance and adsorbate-adsorbate interactions occur at these high lysine loadings.

As suggested by Carta et al.[8] a heterogeneous ion-exchange model can be used for an empirical description of these effects. Following the formulation of Melis et al.[16] with the assumption that ion exchange occurs on distinct functional groups having different selectivity, ion exchange equilibria are described by the following equations:

$$S^j_{i/H^+} = \left(\frac{q^j_0}{C_0}\right)^{1-z_i} \frac{Y^j_i (X_{H^+})^{z_i}}{(Y^j_{H^+})^{z_i} X_i} \tag{6}$$

$$\sum_{i=1}^{N} Y^j_i = 1, \quad j = 1, 2, \ldots, n \tag{7}$$

Table 1. Selectivity coefficients for ion exchange with H^+.

Species	$\bar{S}_{i/H^+}$	S^1_{i/H^+}	S^2_{i/H^+}
Lys^{++}	5.0 g/cm^3		
Lys^+	0.75	1.5	0.27
NH_4^+	1.5		
K^+	1.9		

where S^j_{i/H^+} is the selectivity coefficient for exchange of ion i and H^+ on group j, $Y^j_i = z_i q^j_i / q^j_0$ is the ionic fraction of ion i on group j, q^j_0 is concentration of groups j and n is the number of functional group types. This model was fitted to the monovalent lysine data assuming $n = 2$ and $q^1_0 = q^2_0 = 0.5\, q_0$. In this case, the average selectivity coefficient $\bar{S}_{i/H^+}$ is given by:[16]

$$\bar{S}_{i/H^+} = \sqrt{S^1_{i/H^+} S^2_{i/H^+}} \tag{8}$$

The fitted values of $S^1_{Lys^+/H^+}$ and $S^2_{Lys^+/H^+}$ are given in Table 1 and the calculated line is shown in Fig. 3b. Clearly, the heterogeneous exchange model provides an improved fit, although a significant algebraic complication is introduced. However, it should be noted that despite the success of the model in fitting the data, the physical meaning is not exactly defined since all potential sources of nonidealities leading to nonconstant selectivity are lumped into the heterogeneous model parameters.

In order to complete the general description of ion exchange equilibria it is necessary to combine the solution equilibrium expressions for lysine and ammonia with those for ion exchange equilibrium. In the general case, the charged lysine species and ammonium ion concentrations are given by:

$$C_{Lys^{++}} = \frac{C_{Lys}}{1 + (K_1/C_{H^+}) + (K_1K_2/C^2_{H^+}) + (K_1K_2K_3/C^3_{H^+})} \tag{9}$$

$$C_{Lys^{+}} = \frac{C_{Lys}}{1 + (C_{H^+}/K_1) + (K_2/C_{H^+}) + (K_2K_3/C^2_{H^+})} \tag{10}$$

$$C_{Lys^{-}} = \frac{C_{Lys}}{1 + (C_{H^+}/K_3) + (C^2_{H^+}/K_2K_3) + (C^3_{H^+}/K_1K_2K_3)} \tag{11}$$

$$C_{NH^+_4} = \frac{C_N}{1 + (K_N/C_{H^+})} \tag{12}$$

where C_{Lys} and C_N are the total lysine and total ammonia concentrations. In turn, these concentrations are bound by the electroneutrality condition, which is given by

$$2C_{Lys^{++}} + C_{Lys^+} + C_{NH^+_4} + C_{K^+} + C_{H^+} = C_{Lys^-} + C_{Cl^-} + C_{OH^-} \tag{13}$$

This equation combined with Eqs. 9–12 can be solved for C_{H^+} if the total lysine, total ammonia, and potassium ion concentrations are known. Once the concentrations of individual charged species are calculated, they can be inserted in Eqs. 1–4 or 6–7 in order to calculate the resin-phase composition.

The solid lines in Fig. 2 show the results of these computations. It can be seen that there is an excellent agreement between experimental and predicted lysine uptake as well as between experimental and predicted solution pH.

Although not shown here, predictions for several other conditions were also successful.[17]

Ion Exchange Kinetics

Batch ion exchange curves showing the solution concentration as a function of time are given in Fig. 4 for the following conditions: uptake of divalent lysine on ammonia form resin (Fig. 4a); adsorption of monovalent lysine on

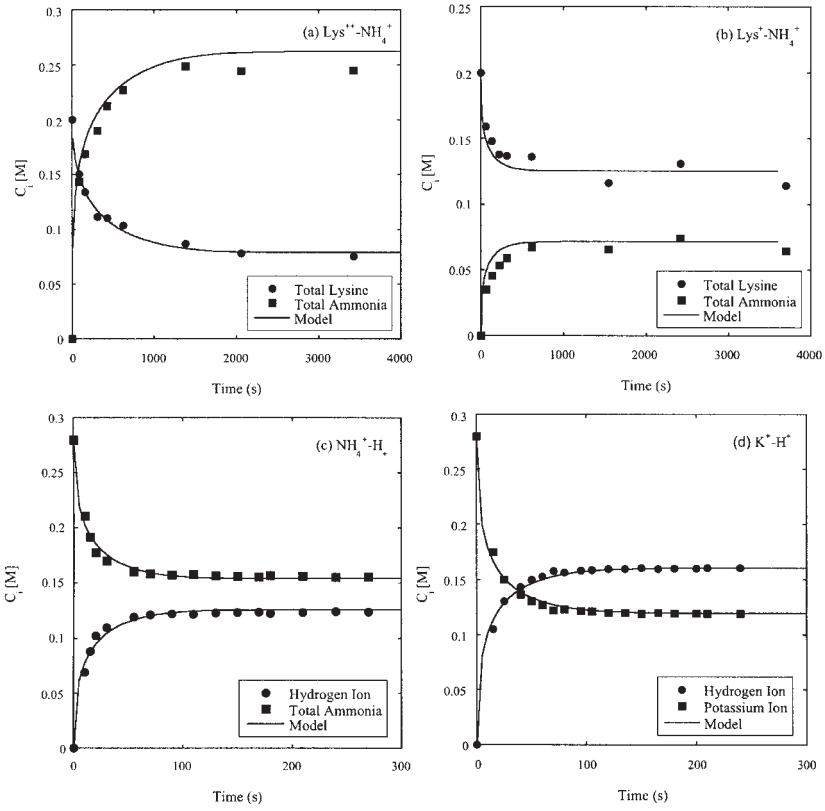

Figure 4. Batch uptake curves for: (a) divalent lysine on ammonia form resin with $C_{Cl^-} = 0.56\,\text{M}$ and $M = 6.0\,\text{g}$; (b) monovalent lysine adsorption on ammonia form resin with $C_{Cl^-} = 0.20\,\text{M}$ and $M = 3.3\,\text{g}$; (c) ammonia adsorption on hydrogen form resin with $C_{Cl^-} = 0.28\,\text{M}$ and $M = 5.1\,\text{g}$; (d) potassium adsorption on hydrogen form resin with $C_{Cl^-} = 0.28\,\text{M}$ and $M = 2.0\,\text{g}$.

ammonia form resin (Fig. 4b); adsorption of ammonia on hydrogen form resin (Fig. 4c); and adsorption of potassium on hydrogen form resin (Fig. 4d). Experiments were conducted with a minimum of two different ratios of the resin mass to solution volume and yielded consistent results.[17] The most noticeable effect is the large difference in the rate of ion exchange, which is slowest for the divalent lysine-ammonia exchange (Fig. 4a) and fastest for the potassium ion-hydrogen ion exchange (Fig. 4d). It should be noted that the divalent lysine experiment actually involves the exchange of the three species Lys^{++}, NH_4^+, and H^+ since the pH is ultimately quite low.

For these fairly concentrated solutions and with the relatively large size of the Dowex HCR-W2 particles, the kinetics of ion exchange can be assumed to be controlled by intraparticle diffusion.[10,11] The following equations and boundary conditions can thus be used to describe the ion exchange kinetics.

For the resin beads:

$$\frac{\partial q_{Lys}}{\partial t} = \frac{1}{r^2}\frac{\partial}{\partial r}\left[r^2(J_{Lys^+} + J_{Lys^{++}})\right] \tag{14}$$

$$\frac{\partial q_N}{\partial t} = -\frac{1}{r^2}\frac{\partial}{\partial r}[r^2(J_{NH_4^+} + J_{NH_3})] \tag{15}$$

$$\frac{\partial q_{K^+}}{\partial t} = \frac{1}{r^2}\frac{\partial}{\partial r}[r^2(J_{K^+})] \tag{16}$$

$$r = 0, \frac{\partial q_{Lys}}{\partial r} = \frac{\partial q_N}{\partial r} = \frac{\partial q_{K^+}}{\partial r} = 0 \tag{17}$$

$$r = r_p, q_{Lys} = q^*_{Lys}, q_N = q^*_N, q_{K^+} = q^*_{K^+} \tag{18}$$

$$t = 0, q_{Lys} = q^0_{Lys}, q_N = q^0_N, q_{K^+} = q^0_{K^+} \tag{19}$$

where

$$q_{Lys} = q_{Lys^+} + q_{Lys^{++}} \tag{20}$$

$$q_N = q_{NH_4^+} + q_{NH_3} \tag{21}$$

$$q_0 = q_{H^+} + q_{K^+} + q_{NH_4^+} + q_{Lys^+} + 2q_{Lys^{++}} \tag{22}$$

For the solution:

$$\frac{dC_{Lys}}{dt} = -\frac{3M}{Vr_p}(J_{Lys^{++}} + J_{Lys^+})|_{r=r_p} \tag{23}$$

$$\frac{dC_N}{dt} = -\frac{3M}{Vr_p}(J_{NH_4^+} + J_{NH_3})|_{r=r_p} \tag{24}$$

$$\frac{dC_{K^+}}{dt} = -\frac{3M}{Vr_p}(J_{K^+})|_{r=r_p} \tag{25}$$

$$t = 0, \quad C_{Lys} = C^0_{Lys}, C_N = C^0_N, C_{K^+} = C^0_{K^+} \tag{26}$$

In these equations, r_p is the particle radius, q_i^* and q_i^0 are the interfacial and initial resin compositions, respectively, M is the mass of resin, V is the solution volume, and the C_i^0 is the initial solution concentrations. According to the Nernst-Planck model, the counterion fluxes and electrostatiscally coupled and can be expressed as[11]

$$J_i = \frac{1}{z_i}\sum_{j=1}^{N} z_j D_{i,j}\frac{\partial q_j}{\partial r} \tag{27}$$

where N is the number of counterions and:

$$D_{i,j} = -\frac{D_i(D_j - D_N)z_i^2 q_i}{\sum_{k=1}^{N} z_k^2 D_k q_k} \quad \text{for } i \neq j \tag{28}$$

$$D_{i,i} = D_i - \frac{D_i(D_i - D_N)z_i^2 q_i}{\sum_{k=1}^{N} z_k^2 D_k q_k} \quad \text{for } i = j \tag{29}$$

D_N is the diffusivity of a reference counterion, e.g., H^+. These equations neglect the presence of zwitterionic and negatively charged lysine in the resin, as these species are expected to be largely excluded due to steric and Donnan potential effects. Unprotonated ammonia, however, is considered. Its effect was not important in the batch experiments, but was found to be significant in column experiments as discussed in part II of this paper. Thus, it is included for completeness.

In the following discussion we consider the special case of simultaneously diffusing lysine, ammonia, and hydrogen ion, which is relevant to the experiments in Fig. 4. For this system it should be recognized that dissociation of divalent lysine could also occur in the resin phase. Combining the expressions for the selectivity coefficient for divalent and monovalent lysine (Eqs. 1 and 2) with the expression for the dissociation constant of divalent lysine in solution we obtain:

$$K_1' = K_1\frac{S_{Lys^+/H^+}}{S_{Lys^{++}/H^+}} = \frac{q_{Lys^+}q_{H^+}}{q_{Lys^{++}}} \tag{30}$$

Using the known pK_1-value and the average selectivity coefficient values and converting $S_{Lys^{++}}/H^+$ to a volume/volume basis using the resin density, we obtain $pK_1' = 3.00$. This represents the dissociation constant for divalent lysine in the resin phase. It is somewhat different from the value in solution, but this can be expected because of the high ion concentration in the resin

phase and the effects of the elastic polyelectrolyte matrix, In any case, this relationship introduces a further coupling of diffusion fluxes, which can be handled as discussed by Hwang and Helfferich[18] for the general case of ion exchange accompanied by fast reversible reactions. By combining Eq. 30 with Eqs. 22 and 20, we obtain:

$$q_{Lys^{++}} = \frac{(q_0 - q_{NH_4^+})q_{Lys^+} - q_{Lys^+}^2}{K_1' + 2q_{Lys^+}} \tag{31}$$

$$q_{Lys} = q_{Lys^+} + \frac{(q_0 - q_{NH_4^+})q_{Lys^+} - q_{Lys^+}^2}{K_1' + 2q_{Lys^+}} \tag{32}$$

In turn, these relationships can be used to express the partial derivatives of q_{Lys} and $q_{Lys^{++}}$ appearing in Eqs. 14 and 27 in terms of q_{Lys^+}. For brevity, the final equations are omitted but can be found in Ref.[17]. The resulting equations were solved numerically to obtain the concentrations of ammonium ion and monovalent lysine in the resin. We used a finite difference method described in Ref.[19] to discretize the partial differential equations and subroutine DIVPAG of the IMSL Mathematical and Statistical Libraries (Visual Numerics, Inc., San Ramon, CA) to solve the resulting system of ordinary differential equations. This subroutine used Gear's method for stiff systems of equations. The interfacial composition was calculated at each integration step by calculating the solution pH and equilibrium composition as previously described.

Individual diffusivities in the resin were determined by fitting the numerical solution of these equations to the experimental data and are given in Table 2. In order to reduce the fitting problem to a single parameter, the hydrogen ion diffusivity, D_{H^+}, was assumed to be $1 \times 10^{-5}\,cm^2/s$ according to literature data for 8% DVB cation exchange resins (see Ref.[9]). As seen in Table 2, the diffusivity of divalent lysine is much smaller than that of monovalent lysine, which is consistent with the behavior of divalent inorganic ions.

Table 2. Diffusion coefficients in solution and resin phase.

Species	D_i^0 ($10^{-5}\,cm^2/s$)	D_i ($10^{-6}\,cm/s$)	D_i/D_i^0
Lys^{++}	0.69[(a)]	0.050	0.0070
Lys^+	0.69[(a)]	0.20	0.029
NH_4^+	1.6[(b)]	1.8	0.095
K^+	2.0[(b)]	1.6	0.11

[(a)]Estimated from Wilke-Chang equation.
[(b)]Ref.[13].

In turn, the diffusivity of monovalent lysine is much smaller than that of ammonium and potassium ion. This occurs because of the large size of the lysine molecule, which causes its diffusion in the resin to be severely hindered. The ratio D_i/D_i^0 is also shown in Table 2 along with the solution diffusivities, This ratio is about $1/200$ for divalent lysine and about $1/30$ for the monovalent form. The latter is consistent with the behavior of other monovalent amino acids.[9] For the smaller inorganic cations, ammonium and potassium, the ratio D_i/D_i^0 is about $1:10$ as there is much less diffusional hindrance for these species than there is for the bulkier lysine molecule.

Finally, the lines in Fig. 5 show model predictions without further adjustment of the diffusivities for two rather different conditions. In the first, divalent and monovalent lysine forms are present simultaneously, while in the second divalent lysine and hydrogen ion and desorbed with ammonia at high pH. In both cases, the ion exchange process involves multicomponent diffusion. The agreement between these experimental results (as well other discussed in Ref.[17]) and the model predictions is not perfect, but it is still adequate for practical purposes, indicating that the model captures the essential characteristics of coupled transport in this complex system.

CONCLUSIONS

Equilibrium and kinetic parameters for the ion exchange of lysine on a strong acid cation exchanger were obtained along with models to describe the dynamics of batch adsorption and desorption. Ion exchange equilibria are described by taking into account the dissociation of protonated lysine species in solution and in the resin phase and expressed in terms of ionic fractions of the counterions. The selectivity coefficients for different binary exchange systems were found to be fairly constant, so that equilibria could be modeled using the mass action law. An exception was the case of monovalent lysine at high resin loading, where the selectivity coefficient appears to decrease substantially as the lysine loading approaches the total ion exchange capacity. This effect can be attributed to steric and size exclusion factors and can be described empirically with a heterogeneous ion exchange equilibrium model. The intraparticle diffusivities determined from batch experiments for ammonium ion and potassium ion found in this work are consistent with literature values.[11] Moreover, the diffusivity of monovalent lysine appears consistent with predictions based on the correlation of Jones and Carta.[9] A much lower diffusivity is found for divalent lysine. Since diffusion in gel-type resins like the one considered in this work occurs through gel pores in close proximity to the charged functional groups bound to the polymeric backbone, it is not surprising that diffusion divalent lysine is

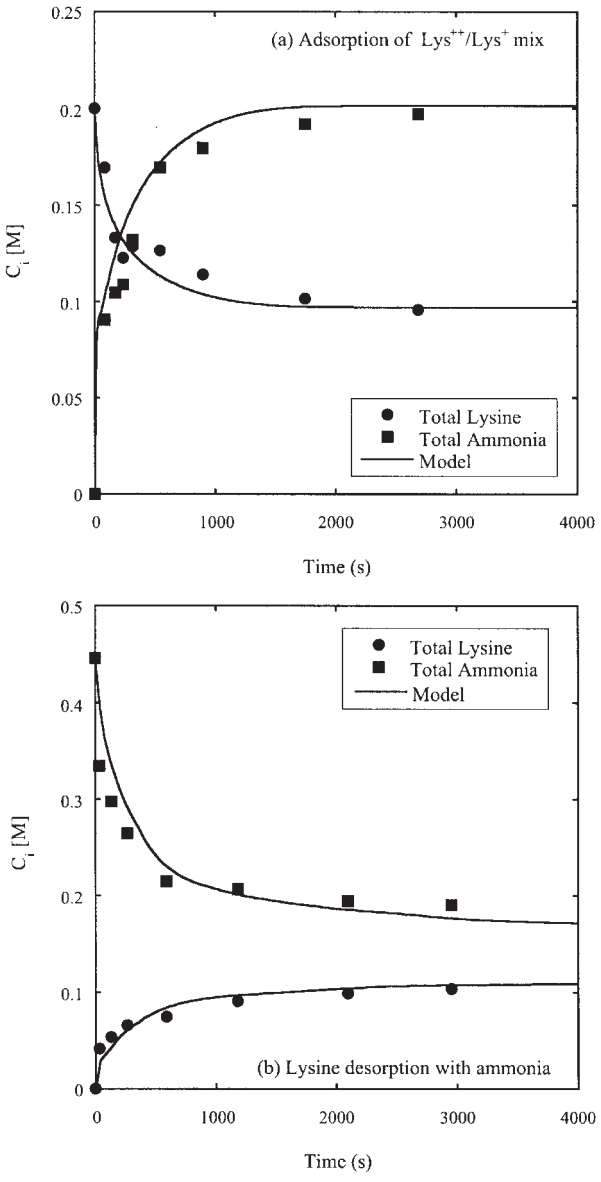

Figure 5. Comparison of experimental and predicted batch ion exchange curves for: (a) divalent and monovalent lysine adsorption on ammonia form resin with $C_{Cl^-} = 0.35$ M and $M = 4.6$ g; (b) desorption of lysine from divalent lysine loaded resin with 0.45 M ammonia and $M = 6.3$ g.

much slower than the monovalent form since the former is likely to interact more strongly with the resin's functional groups. The general kinetic model developed in this work was also found consistent with more complicated cases involving multicomponent transport with the simultaneous presence of divalent and monovalent lysine forms and for desorption. Thus, it can of used to predict batch adsorption under a broad range of conditions. Applications of the results of these studies to fixed-bed behavior are discussed in Part II of this work.

NOMENCLATURE

C_i	concentration of species i in solution (mol/L)
C_0	total co-ion concentration (mol/L)
K_1, K_2, K_3	lysine dissociation constants (mol/L)
K_1'	resin phase dissociation constant for divalent lysine (mol/L)
K_N	ammonia dissociation constant (mol/L)
D_i	resin phase diffusivity of species i (cm^2/s)
D_i^0	solution diffusivity of species i (cm^2/s)
M	resin mass (g)
q_i	concentration of species i in resin phase (mmol/g)
q_0	resin ion exchange capacity (mequiv/g)
r	particle radial coordinate (cm)
r_p	particle radius (cm)
$S_{i/j}$	selectivity coefficient of the exchange of ion i and j
t	time (s)
V	solution volume (mL)
X_i	ionic fraction of species i in solution phase
Y_i	ionic fraction of species i in resin phase
z_i	ion charge

ACKNOWLEDGMENT

This research was supported by Ajinomoto Co., Inc.

REFERENCES

1. Blanch, H.W.; Clark, D.S. *Biochemical Engineering*; Marcel-Dekker, Inc.: New York, 1997.

2. Dye, S.R.; DeCarli II, J.P.; Carta, G. Equilibrium adsorption of amino acids by a cation-exchange resin. Ind. Eng. Chem. Research **1990**, *29*, 849–857.
3. Saunders, M.S.; Vierow, J.B.; Carta, G. Uptake of phenylalanine and tyrosine by a strong acid cation exchanger. AIChE J. **1989**, *35*, 53–68.
4. Jones, I.L.; Carta, G. Ion exchange of amino acids and dipeptides on cation exchange resins with varying degree of crosslinking. 1. Equilibrium. Ind. Eng. Chem. Research **1993**, *32*, 107–117.
5. Carta, G.; Dinerman, A.A. Displacement chromatography of amino acids: Effects of selectivity reversal. AIChE J. **1994**, *40*, 1618–1628.
6. Melis, S.; Markos, J.; Cao, G.; Morbidelli, M. Separation between amino acids and inorganic ions through ion exchange: development of a lumped model. Ind. Eng. Chem. Research **1996**, *35*, 3629–3636.
7. Bellot, J.C.; Tarantino, R.V.; Condoret, J.-S. Thermodynamic modeling of multicomponent ion-exchange equilibria of amino acids. AIChE J. **1999**, *45*, 1329–1341.
8. Carta, G.; Saunders, M.S.; DeCarli II, J.P.; Vierow, J.B. Dynamics of fixed bed separations of amino acids by ion exchange. AIChE Symp. Ser. **1988**, *84*, 54–61.
9. Jones, I.L.; Carta, G. Ion exchange of amino acids and dipeptides on cation exchange resins with varying degree of crosslinking. 2. Intraparticle transport. Ind. Eng. Chem. Research **1993**, *32*, 117–125.
10. Helfferich, F. *Ion Exchange*; McGraw-Hill: New York, NY, 1962.
11. LeVan, M.D.; Carta, G.; Yon, C. Adsorption and Ion Exchange. Section 16. In *Perry's Chemical Engineers' Handbook*, 7th Ed.; Green, D.W., Ed.; McGraw-Hill: New York, 1997.
12. Kawakita, T.; Ogura, T.; Saeki, M. Selectivity coefficient of lysine for strong cation exchange resin of the ammonium form. Agric. Biol. Chem. **1989**, *53*, 2571–2577.
13. Cussler, E.L. *Diffusion—Mass Transfer in Fluid Systems*, 2nd Ed.; Cambridge University Press: Cambridge, UK, 1997.
14. Kawakita, T.; Ito, Y.; Sano, C.; Ogura, T.; Saeki, M. Breakthrough curve of lysine on a column of a strong cation exchange resin of the ammonium form. Sep. Sci. Technol. **1991**, *26*, 619–635.
15. Weast, R.C. *CRC Handbook of Chemistry and Physics*, 59th Ed.; CRC Press: Boca Raton, FL, 1978.
16. Melis, S.; Cao, G.; Morbidelli, M. A new model for the simulation of ion exchange equilibria. Ind. Eng. Chem. Research **1995**, *34*, 3916–3924.
17. Nagai, H. *Model Development and Simulation of Lysine Ion Exchange in Single and Multicolumn Systems*; University of Virginia: Charlottesville, Virginia, 2003; Ph.D. Thesis.

18. Hwang, Y.L.; Helfferich, F.G. Generalized model for multispecies ion exchange kinetics including fast reversible reactions. React. Polym. **1987**, *5*, 237–253.
19. Carta, G.; Lewus, R.K. Film model approximation for particle-diffusion-controlled multicomponent ion exchange. Sep. Sci. Technol. **1999**, *34*, 2685–2697.

Received March 2, 2004
Accepted September 14, 2004